# Strongly convergent method to solve one-dimensional quantum problems

Rubicelia Vargas, Jorge Garza, and Alberto Vela
*Departamento de Química, División de Ciencias Básicas e Ingeniería, Universidad Autónoma Metropolitana-Iztapalapa, Apartado Postal 55-534, México, Distrito Federal 09340, Mexico*
(Received 9 December 1994; revised manuscript received 14 June 1995)

An algorithm to solve the one-dimensional Schrödinger equation subject to Dirichlet boundary conditions is presented. The algorithm is based on a set of theorems that guarantee that when one solves the Schrödinger equation for a confined system and allows the boundaries to increase, the solutions converge strongly, in the norm of Hilbert space $L_2(-\infty,\infty)$, to the exact solutions of the unbounded problem. For the calculation of the solutions of the confined system we use a very efficient matrix method. By applying the algorithm to the harmonic oscillator and to the quartic and sextic potentials we show that with this method one can calculate the eigenvalues and eigenfunctions of a nonbounded one-dimensional problem with a high degree of accuracy and with very reasonable computational effort. We show that the eigenvalues corresponding to the sextic potential, $V(x)=\frac{1}{2}x^2+\alpha_2 x^4+\alpha_3 x^6$, for different values of the parameter $\alpha_3$ behave in a similar fashion as that described by Hioe *et al.* [Phys. Rep. **43C**, 305 (1978)] for the quartic oscillator.

PACS number(s): 02.70.Bf, 03.65.Ge, 02.60.Lj

## I. INTRODUCTION

The exact numerical solution of the one-dimensional Schrödinger equation is relevant in several areas of physics ranging from nonlinear field theory [1] to molecular vibrations [2]. In particular, the class of potentials

$$V(x)=\sum_{k=1}^{M}\alpha_k x^{2k} \tag{1.1}$$

that are defined in the Hilbert space $L_2(-\infty,\infty)$ have received a great deal of attention mainly due to the fact that the Rayleigh-Schrödinger perturbation series for the quartic potential

$$V(x)=\tfrac{1}{2}x^2+\alpha_2 x^4 \tag{1.2}$$

is divergent [3]. Several analytical and numerical approaches have been attempted to solve the Schrödinger equation for this potential [3–18]. The numerical methods employed to solve this problem can be classified according to their need to select an *ad hoc* basis set. Among those that require a basis we can mention the perturbative and variational methods. We can further classify the numerical methods that do not use a basis as (i) shooting (or integration) and (ii) matrix (or global) methods [17–23]. The basic idea in the shooting methods is to discretize the real axis, select an initial estimate of the eigenvalues, and, by inward and outward integration, to iteratively refine the eigenvalue. In the matrix methods, space is also discretized but by writing the problem in matrix form one realizes that the matrices involved for some operators have particular symmetries. Thus, by exploiting these symmetries, it is possible to design an efficient algorithm to find the solution of the problem. It is important to note that these matrix methods we are referring to are not matrix representations of the Hamiltonian. An advantage of the matrix methods is that one does not need an initial guess to start to solve the problem.

When the potential is defined in $L_2(-\infty,\infty)$ either method, shooting or matrix, requires the specification of an additional quantity. This quantity is the *practical infinity,* that is, the value selected *ad hoc* to represent the infinity. Typically [23–25], this point is "judiciously" selected and it is kept fixed after solving the problem for some set of eigenstates. Usually, there is a compromise in the selection of a fixed practical infinity. On one hand, it has to be "large enough" to avoid the artificial lifting of the eigenvalues, and, on the other hand, it has to be "small enough" to overcome the instabilities associated with the numerical integration. An intrinsic limitation of this approach is that if one wishes to obtain the solutions of highly excited states or for a completely different family of potentials it is strictly necessary to tune the selection again. To overcome some of these difficulties, Killingbeck [26] has put forward the idea of using a "floating" infinity to solve the one-dimensional Schrödinger equation by the finite differences method.

Several authors [27–30] have noted that, by confining the system and allowing the boundaries to increase, the solutions of the bounded system converge smoothly to those corresponding to the unbounded one. For confined central-field systems [31], it has been proved that the energy is a decreasing monotonic function of the size of the confining interval. Very recently, Nuñez [32–36] has provided a rigorous mathematical foundation to these facts by stating and proving a set of theorems, the increasing boundaries theorems, that guarantee the convergence of the confined solution to the unbounded one.

In this work we present an algorithm to find the solutions of the one-dimensional Schrödinger equation in $L_2(-\infty,\infty)$. The algorithm combines a fast matrix method [37,38] that solves the Dirichlet problem

 

$$-\frac{1}{2}\frac{d^2\Psi(x)}{dx^2}+[V(x)-E(R)]\Psi(x)=0, \quad x\in(-R,R) ,$$

$$\Psi(-R)=\Psi(R)=0, \quad R=(\text{finite}) , \tag{1.3}$$

and the increasing boundaries theorems. The procedure described in this work has several advantages. First, since it is a matrix method, it requires neither a basis nor a set of test eigenvalues to "shoot" the method. Second, the implementation of the increasing boundaries theorems avoids the problem of practical infinity selection.

The structure of this work is as follows. In Sec. II we present some basic concepts and those aspects of the increasing boundaries theorems which are relevant to the present work. A detailed description of the matrix method used to solve the Dirichlet problem, Eq. (1.3), is presented in Sec. III. The implementation of the increasing boundaries theorems is presented in Sec. IV. To show the convergence and the stability of the method, in Sec. V we apply the algorithm to the harmonic and quartic oscillators, where analytical and very accurate numerical solutions, respectively, are known. The application to the sextic oscillator for different sets of the anharmonic parameters is also presented in Sec. V. The conclusions are given in Sec. VI.

## II. THE INCREASING BOUNDARIES THEOREMS

In this section we present some basic concepts and a summary, without proof, of the increasing boundaries theorems. For the proofs, the reader is referred to Refs. [32–36].

The eigenfunctions of the one-dimensional Schrödinger equation in a bounded region $[-R,R]$ belong to a Hilbert space $L_2(-R,R)$. The natural definition of the inner product in this space is

$$\langle\varphi|\Psi\rangle_R=\int_{-R}^{R}dx\,\varphi^*(x)\psi(x) , \tag{2.1}$$

for any $\varphi,\psi\in L_2(-R,R)$. Provided with a definition for the inner product, it is straightforward to introduce the concepts of norm

$$\|\varphi\|_R=\langle\varphi|\varphi\rangle_R^{1/2} \tag{2.2}$$

and distance

$$d_R(\varphi,\psi)=\|\varphi-\psi\|_R , \tag{2.3}$$

in $L_2(-R,R)$, where $\varphi$ and $\psi$ are any two elements that belong to this Hilbert space.

Due to the completeness of $L_2(-R,R)$, any convergent sequence $\{\varphi_n\}_{n=1}^{\infty}$ in this Hilbert space converges in the sense of Cauchy, i.e.,

$$\lim_{n\to\infty}\|\varphi_n-\varphi_{n-1}\|_R=0 . \tag{2.4}$$

Another convergence criterion is the convergence in the norm: the infinite sequence $\{\varphi_n\}_{n=1}^{\infty}$ converges in the norm to the limit function $\varphi\in L_2(-R,R)$ if

$$\lim_{n\to\infty}\|\varphi_n-\varphi\|_R=0 . \tag{2.5}$$

The latter sequence is called a convergent sequence and this type of convergence is usually referred to as strong convergence [39]. As is shown in any mathematical analysis textbook [40], a convergent sequence is a Cauchy sequence. From the numerical analysis point of view, Cauchy's criterion is an invaluable tool to analyze the behavior of any numerical method that attempts to solve the Schrödinger equation since, in general, the exact solution $\varphi$ is not known.

If we have a sequence of operators $\{\hat{T}_k\}$ which are mappings from a Hilbert space $H_1$ to a Hilbert space $H_2$, we say that the sequence converges strongly to the operator $\hat{T}$ if

$$\lim_{k\to\infty}\|\hat{T}_k\varphi-\hat{T}\varphi\|=0 \quad \forall\ \varphi\in H . \tag{2.6}$$

It is important to remark that the norm in Eq. (2.6) corresponds to that defined in the range of the operators and not to the norm of an operator. For self-adjoint operators one can define a similar convergence criterion, namely, the strong convergence in the generalized sense [32–36].

Turning to the increasing boundaries theorems, we now state without proof the propositions more relevant to this work. The reader is referred to Refs. [32–36] for a detailed presentation and proofs of this subject.

We will denote as $\hat{H}$ and $\hat{H}_R^0$ the Hamiltonian operators associated with the following Schrödinger equations:

$$\hat{H}\Psi=-\frac{1}{2}\frac{d^2\Psi}{dx^2}+V(x)\Psi=E\Psi, \quad x\in(-\infty,\infty) \tag{2.7}$$

with boundary conditions

$$\Psi(-\infty)=\Psi(\infty)=0 ,$$

and

$$\hat{H}_R^0\Psi_R=-\frac{1}{2}\frac{d^2\Psi_R}{dx^2}+V(x)\Psi_R=E_R\Psi_R, \quad x\in(-R,R) \tag{2.8}$$

with boundary conditions

$$\Psi_R(-R)=\Psi_R(R)=0 . \tag{2.9}$$

The operators $\hat{H}$ and $\hat{H}_R^0$ are defined in different Hilbert spaces, and to compare them it is necessary to introduce a new Hamiltonian operator $\hat{H}_R$ that has the same spectrum and eigenfunctions as $\hat{H}_R^0$ and which is self-adjoint in $L_2(-\infty,\infty)$. To proceed further we have to identify each $\Psi\in L_2(-R,R)$ with an element in $L_2(-\infty,\infty)$ that is defined as

$$\Psi(x)=\begin{cases}\Psi(x), & x\in(-R,R)\\ 0 \quad \text{otherwise} .\end{cases} \tag{2.10}$$

Thus the Hamiltonian $\hat{H}_R$ is the direct sum of $\hat{H}_R^0$ and the zero operator which is defined on the orthogonal complement of $L_2(-R,R)$ in $L_2(-\infty,\infty)$. In this way, the spectrum of $\hat{H}_R$ is the same as that of $\hat{H}_R^0$ with the possible addition of zero as an eigenvalue. Both operators have the same set of eigenfunctions.

With the above definitions and results it is possible to show that, if we allow the boundaries to increase, that is, if we let $R \to \infty$, then the sequence $\{\hat{H}_R\}_R$ converges strongly (in the generalized sense) to the operator $\hat{H}$, i.e.,

$$\lim_{R\to\infty} \|\hat{H}_R\Psi - \hat{H}\Psi\| = 0 , \tag{2.11}$$

where $\Psi \in C_0^\infty(-\infty,\infty)$.

This strong convergence in the generalized sense has several consequences [32–36]. Below we present those that have a direct impact in this work.

(i) If $E_i(R)$ and $E_j(R)$ are the eigenvalues corresponding to two different eigenstates ($i \neq j$) of Eq. (2.8), then their graphs never intersect.

(ii) The functions $E_i(R)$ are nonincreasing.

(iii) If $E_i$ is the exact eigenvalue of the $i$th eigenstate of the unbounded Hamiltonian Eq. (2.7), then $E_i$ is a horizontal asymptote of the curve $E_i(R)$.

The previous propositions lead to the first increasing boundaries theorem.

(IBT 1) *Let $E_i(R)$ and $E_i$ be isolated eigenvalues of $\hat{H}_R^0$ and $\hat{H}$, respectively. Then there exists at least one sequence $\{E_i(R)\}$ that converges to $E_i$ and satisfies $E_i(R) \geq E_i$ for any $R$.*

By invoking the concept of stability it is possible to state the second increasing boundaries theorem.

(IBT 2) *Let $E_i$ be an isolated eigenvalue of $\hat{H}$ and $E_i(R)$ the unique curve asymptotic to $E_i$. Then $E_i$ is stable with respect to the sequence $\{\hat{H}_R\}_R$. In particular, if $E_i(R)$ and $\Psi_i^R(x)$ are the eigenvalue and eigenfunction, respectively, of $\hat{H}_R^0$, then the sequence $\{\Psi_i^R(x)\}_R$ converges in the norm of $L_2(-\infty,\infty)$ to the eigenfunction associated with $E_i$.*

It is important to note, as has been clearly remarked by Nuñez [32–36], that all the statements made in this section are completely independent of the numerical method employed to solve the Dirichlet problem, Eqs. (2.8) and (2.9).

## III. MATRIX FORMULATION OF NUMEROV'S METHOD

In this section we review Lindberg's matrix approach [37,38] to find the solutions of the bounded one-dimensional Schrödinger equation with Dirichlet's boundary conditions. We end the present section by demonstrating that the numerical solutions obtained by this method converge in the norm to the exact solutions.

To solve the one-dimensional Schrödinger equation (1.3), Lindberg discretizes Numerov's method [24] using an equally spaced mesh with step

$$h = \frac{2R}{N+1} , \tag{3.1}$$

where $N$ is the number of internal points in the grid, and such that $x = x_k - R + kh$. This leads to the expression

$$\frac{\Psi_{k-1} - 2\Psi_k + \Psi_{k+1}}{h^2} - \frac{1}{12}[P_{k-1}\Psi_{k-1} + 10P_k\Psi_k + P_{k+1}\Psi_{k+1}] + \frac{\lambda}{12}[\Psi_{k-1} + 10\Psi_k + \Psi_{k+1}] = -\frac{h^2}{240}\Psi_k^{(6)} + \cdots , \tag{3.2}$$

where $P_k = P(x_k) = 2V(x_k)$ and $\lambda = 2E$. By setting the right hand side of Eq. (3.2) equal to zero, we arrive at the starting equation of Lindberg's matrix method. Note that Dirichlet's boundary conditions imply that

$$\Psi_0 = \Psi_{N+1} = 0 . \tag{3.3}$$

The resulting generalized eigenvalue problem can be written in matrix form as

$$A\Psi + \lambda M\Psi = 0 , \tag{3.4}$$

where $A$ and $M$ are the tridiagonal matrices

$$A = \text{trid}\left[1 - \frac{h^2}{12}P_{k-1}, -2 - \frac{10}{12}h^2P_k, 1 - \frac{h^2}{12}P_{k+1}\right] , \tag{3.5}$$

$$M = \frac{h^2}{12}\text{trid}(1,10,1) , \tag{3.6}$$

respectively, and $\Psi$ is the column vector

$$\Psi = \begin{bmatrix} \Psi_0 = \Psi(-R) = 0 \\ \Psi_1 \cong \Psi(-R+h) \\ \vdots \\ \Psi_k \cong \Psi(-R+kh) \\ \vdots \\ \Psi_{N+1} = \Psi(-R) = 0 \end{bmatrix} . \tag{3.7}$$

To find the eigenvalues, Lindberg [37,38] states and proves two theorems. The first theorem establishes that the eigenvalues of Eq. (3.4) are real and located within the interval $[P_{\min} + d_1, P_{\max} + d_N]$ where

$$P_{\substack{\min \\ (\max)}} = \begin{Bmatrix} \min \\ \max \end{Bmatrix}_{1 \leq k \leq N} P_k \tag{3.8}$$

and

$$d_k = \frac{48}{h^2}\frac{\sin^2[k\pi/2(N+1)]}{8 + 4\cos^2[k\pi/2(N+1)]} . \tag{3.9}$$

For practical purposes, instead of the second theorem, the following corollary is used: *the number of eigenvalues associated with Eq. (3.4) that are less than $\theta > 0$ is equal to the number of positive entries in the diagonal matrix $\Delta(\theta)$* (for the details on how to construct the matrix $\Delta(\theta)$, see Refs. [37,38]). Making use of this property, we proceed to the isolation of the total number of eigenvalues ($N_T$) that one wishes to calculate. This is accomplished by successive bisections. After completing this step, we have a set of intervals

$$I_i = [\underline{\varepsilon_i}, \overline{\varepsilon_i}], \quad i = 1,2,\ldots,N_T , \tag{3.10}$$

such that the number of eigenvalues contained inside equal $I_i$ is exactly 1.

To assure the validity of this theorem the step $h$ must satisfy the inequality $h<\sqrt{12/|P_k|}$ for all points in the grid. This sets an upper limit to the value of the step that must be used to guarantee the convergence of the method.

The following step is to reduce the length of each interval. In our approach, we do this by 12 additional bisections. Finally, the eigenvalues are refined by solving the following equation by the secant method:

$$\det\{\Delta(\theta)\}=0, \quad \theta\in I_i \text{ and } i=1,2,\ldots,N_T \; . \tag{3.11}$$

The determinant in Eq. (3.11) is obtained by taking the product of the elements of $\Delta(\theta)$. The accuracy of the eigenvalues obtained by the procedure described above is $h^4$. It is possible to improve this accuracy to $h^8$ by a defect correction calculation [37,38]. This was not done in the present work. For each eigenvalue, the corresponding eigenfunction is obtained by inverse iteration.

We now turn to proving that the numerical solution obtained with the method described in this section converges strongly to the exact solution of the Dirichlet problem, Eq. (2.9), in the limit when $h\to 0$. The proof goes along the lines of that presented in Ref. [41] for the finite differences method.

Rearranging Eq. (3.2) and multiplying by $h^2$ we have that the exact eigenfunction ($\Psi$) and eigenvalue ($\varepsilon$) satisfy the following expression:

$$\left[1-\frac{h^2}{12}P_{k+1}\right]\Psi_{k+1}+\frac{h^2}{12}\varepsilon\Psi_{k+1}+\left[-2-\frac{10}{12}h^2P_k\right]\Psi_k +\frac{10}{12}h^2\varepsilon\Psi_k+\left[1-\frac{h^2}{12}P_{k-1}\right]\Psi_{k-1} +\frac{h^2}{12}\varepsilon\Psi_{k-1}+\frac{h^2}{12}\varepsilon\Psi_k^{(6)}+\cdots=0 \; . \tag{3.12}$$

If we neglect terms of order $h^6$ and higher, we get an expression that provides estimates of the eigenfunctions ($\eta_k\cong\Psi_k$) and eigenvalues ($\theta\cong\varepsilon$). This approximate numerical solution satisfies the equations

$$\left[1-\frac{h^2}{12}P_{i+1}\right]\eta_{i+1}+\frac{h^2}{12}\theta\eta_{i+1}+\left[-2-\frac{10}{12}h^2P_i\right]\eta_i +\frac{10}{12}h^2\theta\eta_i+\left[1-\frac{h^2}{12}P_{i-1}\right]\eta_{i-1} +\frac{h^2}{12}\theta\eta_{i-1}=0 \; . \tag{3.13}$$

Subtracting Eq. (3.13) from Eq. (3.12), introducing the definitions $e_i=\eta_i-\Psi_i$, $a_i=\frac{1}{480}\Psi_i^{(6)}$, $t_i=1-\frac{1}{12}h^2P_i$, and $\nu_i=-2-\frac{10}{12}h^2P_i$, and making use of the fact that the error in the eigenvalues is of order $h^4$, we have that

$$(\nu_i-\tfrac{10}{12}h^2\theta)e_i=(t_{i+1}+\tfrac{1}{12}h^2\theta)e_{i+1}+(t_{i-1}+\tfrac{1}{12}h^2\theta)e_{i-1} +\tfrac{1}{12}Ch^6[\Psi_{i+1}+10\Psi_i+\Psi_{i-1}]+h^6a_i \; , \tag{3.14}$$

where $C$ is the coefficient associated with the error in the eigenvalue. Taking the absolute value of Eq. (3.14) and using the triangle inequality, one gets

$$|\nu_i-\tfrac{10}{12}h^2\theta|\,|e_i| \le|t_{i+1}+\tfrac{1}{12}h^2\theta|\,|e_{i+1}|+|t_{i-1}+\tfrac{1}{12}h^2\theta|\,|e_{i-1}| +\tfrac{1}{12}|C|h^6|\Psi_{i+1}+10\Psi_i+\Psi_{i-1}|+h^6|a_i| \; . \tag{3.15}$$

With $e=\max_i|e_i|$, $a=\max_i|a_i|$, $t=\max_i|t_i+\frac{1}{12}h^2\theta|$, and $\varphi=\max_i|\Psi_i|$, Eq. (3.15) reduces to

$$|\nu_i-\tfrac{10}{12}h^2\theta|\,|e_i|\le 2te+\varphi h^6+ah^6 \; . \tag{3.16}$$

Since

$$|\nu_k-\tfrac{10}{12}h^2\theta|\le 2+\tfrac{10}{12}h^2\max_k|P_k-\theta| \; ,$$

we conclude that

$$|\eta_k-\Psi_k|\le\frac{3}{2}\,\frac{(|C|\varphi+a)h^4}{\max\limits_k|P_k-\theta|} \; . \tag{3.17}$$

Taking the limit when $h\to 0$, we have that

$$\lim_{h\to 0}|\eta_k-\Psi_k|=0 \; , \tag{3.18}$$

showing that locally the numerical solution converges *strongly* to the exact solution of the bounded problem and that the local error is of order $h^4$.

Squaring Eq. (3.17), multiplying by $\Delta x$, and summing over all points $k$ in the grid, we obtain that

$$\|\eta(x)-\Psi(x)\|\le\frac{3}{2}\sqrt{2R}\,\frac{|\,|C|\varphi+a\,|h^4}{\max\limits_k|P_k-\theta|} \; . \tag{3.19}$$

If we take the limit of vanishing $h$ in Eq. (3.19), we finally obtain that

$$\lim_{h\to 0}\|\eta(x)-\Psi(x)\|=0 \; . \tag{3.20}$$

Thus we have proved that the numerical solution $\eta(x)$ of the Dirichlet problem converges in the norm to the exact solution of the bounded problem. This result is a direct consequence of the fact that strong convergence implies convergence in the norm.

## IV. INCREASING BOUNDARIES ALGORITHM

The increasing boundaries theorems (see Sec. II) immediately suggest a numerical procedure to solve the one-dimensional Schrödinger equation associated with an unbounded problem. This can be clearly seen by noting that the increasing boundaries theorems and Eq. (3.20) imply that the exact solution $\psi_i(x)$ of the unbounded system is obtained when

$$\lim_{R\to\infty}\lim_{h\to 0}\|\varphi_i^{(R,h)}(x)-\psi_i(x)\|_\infty=0 \; , \tag{4.1}$$

where $\varphi_i^{(R,h)}(x)$ is the approximate numerical eigenfunction [$\eta(x)$ in Eq. (3.20)] of the confined problem, corresponding to step $h$.

In this section we present an algorithm, which we will call the increasing boundaries algorithm (IBA), that

merges a numerical implementation of the increasing boundaries theorems (Sec. II) with the matrix approach of Sec. III to solve the Schrödinger equation corresponding to the unbounded problem.

The algorithm is the following. In the first step, an initial value ($R^0$) for the boundaries and a number of points ($N$) are selected. This allows the calculation of the step ($h$) as

$$h=\frac{2R^0}{N+1}\ , \tag{4.2}$$

which will be held constant. The potential $V(x)$ is calculated for all points in the grid and the Dirichlet problem in $(-R^0,R^0)$ is solved using Lindberg's matrix method (see Sec. III). After this step, we have the first approximation to the eigenfunctions and eigenvalues which we will denote as $\{\varphi_i^1(x),\ x\in(-R^0,R^0)\}$ and $\{\varepsilon_i^1\}$, respectively. For the first iteration we define $\{\varphi_i^0(x)=0,\ x\in(-R^0,R^0)\}$ and thus the distance between $\varphi_i^0(x)$ and $\varphi_i^1(x)$ is 1. This can be seen from the expression that we use to calculate the distance between two successive eigenfunctions. Let $\{\varphi_i^M(x),\ x\in(-R^M,R^M)\}$ and $\{\varphi_i^{M+1}(x),\ x\in(-R^{M+1},R^{M+1})\}$, where $R^{M+1}>R^M$, be any two successive solutions of Dirichlet's problem associated with the intervals $(-R^M,R^M)$ and $(-R^{M+1},R^{M+1})$, respectively. To guarantee that the IBA satisfies the conditions set by the increasing boundaries theorems, it is necessary to comply with Eq. (2.10). This leads us to the following expression for the distance between $\varphi_i^M(x)$ and $\varphi_i^{M+1}(x)$:

$$\|\varphi_i^{M+1}-\varphi_i^M\|_\infty=\left[\int_{-R^{M+1}}^{R^{M+1}}dx[\varphi_i^{M+1}(x)]^2+\int_{-R^M}^{R^M}dx[\varphi_i^M(x)]^2-2\int_{-R^M}^{R^M}dx\,\varphi_i^{M+1}(x)\varphi_i^M(x)\right]\ . \tag{4.3}$$

Notice that in Eq. (4.3) we are using the norm in $L_2(-\infty,\infty)$. Thus, from Eq. (4.3) and the definition for $\varphi_i^0(x)$, we have that the distance between $\varphi_i^1(x)$ and $\varphi_i^0(x)$ is 1. Since the desired convergence criterion will always be less than 1, we now proceed to increase the interval. This is done by adding a fixed number of points ($N_p$) beyond the previous limits. The number of points added must be even to assure that the interval is increased symmetrically. Thus the updated values of the boundaries are calculated according to the expression

$$R^M=R^{M-1}+\tfrac{1}{2}N_p h,\quad M=1,2,\ldots\ , \tag{4.4}$$

with a similar expression for the negative part of the interval. Now the Dirichlet problem in the interval $(-R^M,R^M)$ is solved. The distances between the new wave functions $\{\varphi_i^M(x)\}$ and the previous $\{\varphi_i^{M-1}(x)\}$ are calculated according to Eq. (4.3) and when this distance is less than a given tolerance the procedure for the $i$th eigenstate ends.

In the following section we illustrate the application of the IBA to some well known problems.

## V. RESULTS

To show the advantages of the IBA described in the previous section, now we apply it to some well known one-dimensional problems. First we show some features of the method by solving the one-dimensional Schrödinger equation for the harmonic oscillator. Since the solutions of the unbounded harmonic oscillator are known analytically, we can test the behavior, stability, and speed of convergence of the IBA. The second problem to be addressed is that of the quartic potential, Eq. (1.2). As noted in the Introduction, this is a very well studied problem. Due to the fact that the known analytical solutions are not valid for the whole range of values of the coupling parameter $\alpha_2$, it is important to have a reliable numerical method that allows the calculation of the solutions corresponding to any value of the anharmonicity parameter. In the present work we will consider quartic potentials with $\alpha_2>0$. When $\alpha_2$ is positive this potential has only one minimum. This means that in this work we will not study the solutions of symmetrical double wells.

Finally, the sextic potential is considered. The general form of this last potential is

$$V(x)=\alpha_1x^2+\alpha_2x^4+\alpha_3x^6\ . \tag{5.1}$$

There is considerably less work done on this potential. Recently, a perturbative method [6] has been devised to solve the one-dimensional Schrödinger equation for this potential. We will compare our results with those available in the literature.

### A. Harmonic oscillator

In Fig. 1 we present the behavior of the first ten eigenvalues of the harmonic oscillator as a function of the size $(-R^M,R^M)$ of the interval. Three things should be noticed. First, one can see that the exact eigenvalues are asymptotes of the curves $\{\lambda_i(R^M)\}$. The second feature to be noticed is that the curves are nonincreasing. Finally, we see that these curves never cross. These observa-

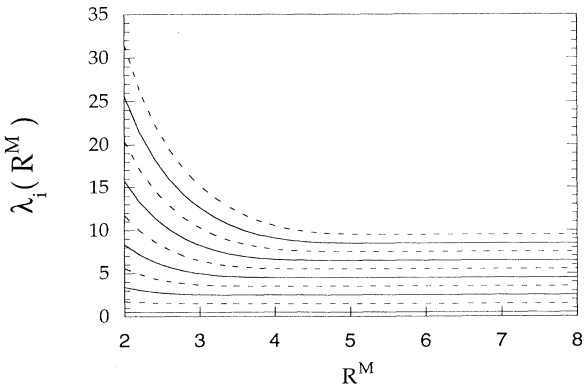


FIG. 1. Eigenvalues of the bounded harmonic oscillator as a function of the size of the confining interval $(-R^M,R^M)$. States with even parity are shown with solid lines and states with odd parity are shown with dashed lines. The step used is $h=0.0025$.

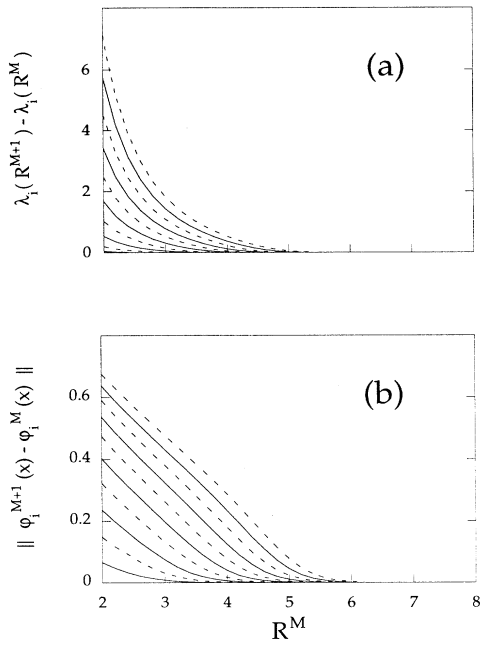


FIG. 2. Convergence of the (a) eigenvalues and (b) eigenfunctions of the bounded harmonic oscillator. Solid lines are used for even states and dashed lines for odd states. The step used is $h=0.0025$.

tions provide numerical evidence for the theorems recently proved by Nuñez that are summarized in Sec. II. To illustrate the convergence of the IBA, in Fig. 2 we present the behavior of the distance between two successive eigenvalues and eigenfunctions with respect to the size of the interval for the first ten states of the harmonic oscillator. The distance was calculated according to Eq. (4.3). From these plots it is clear that the method converges in the sense of Cauchy. By comparing the convergence of the eigenvalues and eigenfunctions, we see that the rate of convergence of the eigenvalues is faster than that corresponding to the eigenfunctions. Thus, by achieving convergence in the eigenfunctions, the convergence of the eigenvalues is automatically guaranteed. Also note that the convergence is slower for the higher excited states than for the lower ones. In other words, more cycles (intervals) are needed to achieve the same quality (convergence threshold) in the solution of an excited state.

To show that the IBA converges in the norm to the exact eigenfunctions of the unbounded problem, in Fig. 3 we depict the behavior of the distance between the solution corresponding to a given $R^M$ and the exact eigenfunction of the unbounded harmonic oscillator. We have found that the curves for two different steps ($h=0.01$ and 0.0025) are practically the same. It is noteworthy that for small confinements the distance of the higher lying excited states shows an oscillatory behavior. From the observation made above in regard to the invariant nature of these plots for two different small steps, we think that this behavior is not due to any numerical instability of the method.

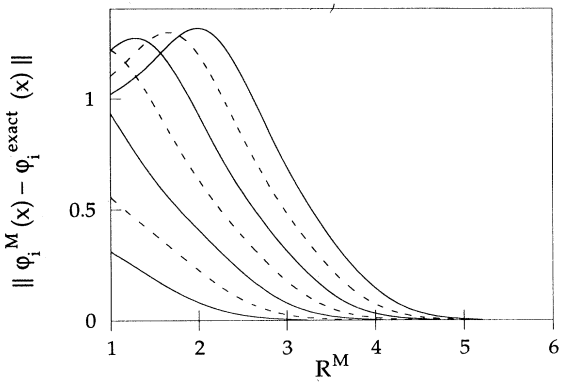


FIG. 3. Convergence in the norm of the eigenfunctions of the bounded harmonic oscillator to the exact eigenfunctions of the unbounded harmonic oscillator. Solid lines are used for even states and dashed lines for odd states. The step used is $h=0.0025$.

The critical parameter in the present method is the step ($h$), which in turn depends on the size of the interval and the number of points in the grid. If $h$ is not small enough, the approximated eigenvalues can go below the exact ones. This is illustrated in Table I where we present results for two different values of $h$. For $h=10^{-2}$, all the approximated eigenvalues, except the ground state, go below the exact value. When $h$ is decreased to $h=2.5\times10^{-3}$, all the low lying states converge from above, and the high lying states are only slightly below the exact eigenvalue. We performed a divided differences analysis for several states of the bounded harmonic oscillator, and for several confinements. The analysis shows that indeed the errors in the eigenvalues provided by the present implementation of Lindberg's matrix method are of order $h^4$. Thus we can write that

$$\lambda_i(h,R)=E_i(R)+C_i(R)h^4 , \tag{5.2}$$

where $\lambda_i(h,R)$ is the approximated eigenvalue $E_i(R)$ is the exact eigenvalue and $C_i(R)$ is the error coefficient. Using the values shown in Table I corresponding to the steps $h_1=0.01$ and $h_2=0.0025$, we can improve the accuracy of the eigenvalues by a Richardson extrapolation, as has been suggested by Killingbeck [26]. The extrapolated values are also shown in Table I. As can be seen, for all the eigenvalues the convergence of the bounded to the unbounded eigenvalues is always from above. This confirms the fact that Numerov's method is exact in the limit $h\rightarrow0$.

Certainly, for a given $h$ there is always one excited state such that its corresponding energy is lower than the exact one. However, the smaller the step, the higher the excited state where this latter behavior will be observed. Thus, if one is interested in the solutions of highly excited states, one should be careful to use a step small enough to assure the convergence from above or to perform a Richardson extrapolation. The behavior described in this paragraph is a consequence of the nonvariational nature of the finite differences method.

TABLE I. Selected eigenvalues of the bounded harmonic oscillator as a function of the size of the interval ($R$) for two different steps ($h$) and the corresponding extrapolated values.

| $R$ | $\lambda_0$ | $\lambda_1$ | $\lambda_2$ | $\lambda_7$ | $\lambda_8$ | $\lambda_9$ |
|---|---|---|---|---|---|---|
| | | | $h=0.01$ | | | |
| 1.0 | 1.298 459 831 3 | 5.075 581 993 5 | 11.258 825 549 6 | 79.121 898 736 7 | 100.095 044 307 9 | 123.535 436 813 6 |
| 2.0 | 0.537 461 209 2 | 1.764 816 438 0 | 3.399 788 236 4 | 20.403 519 392 4 | 25.647 331 111 9 | 31.507 794 442 0 |
| 3.0 | 0.500 391 082 9 | 1.506 081 527 0 | 2.541 127 258 3 | 10.303 784 865 3 | 12.629 086 917 3 | 15.229 385 759 3 |
| 4.0 | 0.500 000 490 8 | 1.500 014 602 7 | 2.500 201 179 0 | 7.793 679 578 8 | 9.091 013 066 2 | 10.533 684 376 6 |
| 5.0 | 0.500 000 000 0 | 1.500 000 003 4 | 2.500 000 083 0 | 7.502 927 978 5 | 8.511 471 285 9 | 9.536 572 922 8 |
| 6.0 | 0.500 000 000 0 | 1.499 999 999 7 | 2.499 999 999 0 | 7.500 001 241 2 | 8.500 008 590 6 | 9.500 049 917 8 |
| 7.0 | 0.500 000 000 0 | 1.499 999 999 7 | 2.499 999 999 0 | 7.499 999 977 6 | 8.499 999 967 8 | 9.499 999 958 1 |
| 8.0 | 0.500 000 000 0 | 1.499 999 999 7 | 2.499 999 999 0 | 7.499 999 977 5 | 8.499 999 967 5 | 0.499 999 954 7 |
| | | | $h=0.0025$ | | | |
| 1.0 | 1.298 459 832 0 | 5.075 582 015 1 | 11.258 825 780 6 | 79.121 980 533 0 | 100.095 210 139 6 | 123.535 748 891 3 |
| 2.0 | 0.537 461 209 3 | 1.764 816 438 8 | 3.399 788 241 1 | 20.403 520 678 5 | 25.647 333 712 4 | 31.507 799 328 2 |
| 3.0 | 0.500 391 082 9 | 1.506 081 527 3 | 2.541 127 259 5 | 10.303 784 985 8 | 12.629 087 155 2 | 15.229 386 200 3 |
| 4.0 | 0.500 000 490 9 | 1.500 014 603 0 | 2.500 201 180 0 | 7.793 679 610 1 | 9.091 013 121 0 | 10.533 684 470 5 |
| 5.0 | 0.500 000 000 1 | 1.500 000 003 7 | 2.500 000 084 0 | 7.502 928 001 0 | 8.511 471 318 9 | 9.536 572 970 3 |
| 6.0 | 0.500 000 000 0 | 1.500 000 000 0 | 2.500 000 000 0 | 7.500 001 263 6 | 8.500 008 623 0 | 9.500 049 962 9 |
| 7.0 | 0.500 000 000 0 | 1.500 000 000 0 | 2.500 000 000 0 | 7.499 999 999 9 | 8.500 000 000 3 | 9.500 000 003 2 |
| 8.0 | 0.500 000 000 0 | 1.500 000 000 0 | 2.500 000 000 0 | 7.499 999 999 9 | 8.499 999 999 9 | 9.499 999 999 8 |
| | | | Extrapolated | | | |
| 1.00 | 1.298 459 832 | 5.075 582 015 | 11.258 825 780 | 79.121 980 212 | 100.095 209 489 | 123.535 747 667 |
| 2.00 | 0.537 461 209 | 1.764 816 439 | 3.399 788 241 | 20.403 520 673 | 25.647 333 702 | 31.507 799 309 |
| 3.00 | 0.500 391 083 | 1.506 081 527 | 2.541 127 259 | 10.303 784 985 | 12.629 087 154 | 15.229 386 199 |
| 4.00 | 0.500 000 491 | 1.500 014 603 | 2.500 201 180 | 7.793 679 610 | 9.091 013 121 | 10.533 684 470 |
| 5.00 | 0.500 000 000 | 1.500 000 004 | 2.500 000 084 | 7.502 928 001 | 8.511 471 319 | 9.536 572 970 |
| 6.00 | 0.500 000 000 | 1.500 000 000 | 2.500 000 000 | 7.500 001 264 | 8.500 008 623 | 9.500 049 963 |
| 7.00 | 0.500 000 000 | 1.500 000 000 | 2.500 000 000 | 7.500 000 000 | 8.500 000 000 | 9.500 000 003 |
| 8.00 | 0.500 000 000 | 1.500 000 000 | 2.500 000 000 | 7.500 000 000 | 8.500 000 000 | 9.500 000 000 |

TABLE II. Selected expectation values $\langle x^2\rangle$ and $\langle x^4\rangle$ for the bounded harmonic oscillator as a function of the size of the interval. The exact analytical values for the unbounded harmonic oscillator are at the bottom of each column. The step used is $h=0.0025$.

| $R$ | $\langle x^2\rangle_0^R$ | $\langle x^4\rangle_0^R$ | $\langle x^2\rangle_1^R$ | $\langle x^4\rangle_1^R$ |
|---|---|---|---|---|
| 1.0 | 0.128 292 527 7 | 0.039 909 928 4 | 0.280 444 849 5 | 0.112 594 404 1 |
| 2.0 | 0.402 907 823 5 | 0.430 814 876 3 | 0.996 219 011 6 | 1.476 106 521 0 |
| 3.0 | 0.497 078 735 8 | 0.733 197 214 5 | 1.461 678 501 5 | 3.477 378 553 0 |
| 4.0 | 0.499 992 836 9 | 0.749 933 768 2 | 1.499 803 064 7 | 3.747 897 747 9 |
| 5.0 | 0.499 999 998 2 | 0.749 999 974 9 | 1.499 999 916 7 | 3.749 998 734 1 |
| 6.0 | 0.500 000 000 0 | 0.750 000 000 0 | 1.500 000 000 0 | 3.749 999 999 9 |
| 7.0 | 0.500 000 000 0 | 0.750 000 000 0 | 1.500 000 000 0 | 3.750 000 000 0 |
| 8.0 | 0.500 000 000 0 | 0.750 000 000 0 | 1.500 000 000 0 | 3.750 000 000 0 |
| Exact | 0.5 | 0.75 | 1.5 | 3.75 |
| $R$ | $\langle x^2\rangle_4^R$ | $\langle x^4\rangle_4^R$ | $\langle x^2\rangle_9^R$ | $\langle x^4\rangle_9^R$ |
| 1.0 | 0.325 734 820 7 | 0.184 473 812 6 | 0.331 473 502 7 | 0.196 103 916 2 |
| 2.0 | 1.331 301 657 9 | 3.011 897 700 2 | 1.335 927 639 0 | 3.169 498 444 4 |
| 3.0 | 3.109 685 667 2 | 15.178 791 394 7 | 3.105 279 815 3 | 16.753 641 255 1 |
| 4.0 | 4.408 517 573 5 | 29.387 679 429 9 | 5.973 801 359 7 | 58.286 882 771 2 |
| 5.0 | 4.499 758 415 4 | 30.745 277 701 4 | 9.090 977 828 0 | 124.853 048 687 7 |
| 6.0 | 4.499 999 960 9 | 30.749 999 017 7 | 9.498 807 538 4 | 135.711 363 135 0 |
| 7.0 | 4.499 999 999 9 | 30.749 999 999 3 | 9.499 999 873 0 | 135.749 995 053 5 |
| 8.0 | 4.499 999 999 9 | 30.749 999 999 3 | 9.499 999 999 5 | 135.749 999 988 7 |
| Exact | 4.5 | 30.75 | 9.5 | 135.75 |

TABLE III. Eigenvalues for the quartic anharmonic potential for different values of the anharmonicity parameter, calculated with a step of $h=0.0025$.

| $\alpha_2$ | $\varepsilon_0$ | $\varepsilon_1$ | $\varepsilon_2$ | $\varepsilon_3$ | $\varepsilon_4$ | $\varepsilon_5$ |
|---|---|---|---|---|---|---|
| 0.0001 | 0.500 074 973 8 | 1.500 374 794 0 | 2.500 974 232 5 | 3.501 873 035 4 | 4.503 070 949 4 | 5.504 567 721 7 |
| 0.001 | 0.500 747 395 6 | 1.503 729 615 7 | 2.509 674 352 7 | 3.518 557 186 8 | 4.530 354 213 7 | 5.545 042 027 5 |
| 0.01 | 0.507 256 204 5 | 1.535 648 278 3 | 2.590 845 796 2 | 3.671 094 942 2 | 4.774 913 118 6 | 5.901 026 674 1 |
| 0.1 | 0.559 146 327 2 | 1.769 502 644 0 | 3.138 624 308 5 | 4.628 882 808 9 | 6.220 300 899 9 | 7.899 767 227 7 |
| | (0.559 146 33)[a] | (1.769 502 6)[a] | (3.138 624)[a] | (4.628 883)[a] | (6.220 30)[a] | |
| | (0.559 146 3)[b] | (1.769 502 6)[b] | (3.138 624 3)[b] | (4.628 882 8)[b] | (6.220 300 9)[b] | (7.899 767 2)[b] |
| 1.0 | 0.803 770 651 2 | 2.737 892 268 0 | 5.179 291 687 6 | 7.942 403 984 2 | 10.963 583 093 7 | 14.203 139 103 6 |
| | (0.803 770 66)[a] | (2.737 892)[a] | (5.179 292)[a] | (7.942 40)[a] | (10.963 58)[a] | |
| 10.0 | 1.504 972 407 8 | 5.321 608 256 2 | 10.347 055 590 0 | 16.090 146 869 4 | 22.408 751 284 6 | 29.211 484 850 8 |
| | (1.504 972)[a] | (5.321 608)[a] | (10.347 06)[a] | (16.090 1)[a] | (22.408 8)[a] | |
| 100.0 | 3.131 384 164 9 | 11.187 254 250 1 | 21.906 898 144 3 | 34.182 524 096 5 | 47.707 205 844 9 | 62.281 237 883 0 |
| | (3.131 384 2)[a] | (11.187 254)[a] | (21.906 90)[a] | (34.182 5)[a] | (47.707 2)[a] | |
| 1 000.0 | 6.694 220 849 7 | 23.972 206 047 4 | 47.017 338 685 9 | 73.419 113 688 7 | 102.516 156 733 8 | 133.876 890 353 7 |
| | (6.694 221)[a] | (23.972 21)[a] | (47.017 34)[a] | (73.419 11)[a] | (102.516)[a] | |
| 10 000.0 | 14.397 995 335 7 | 51.586 103 242 8 | 101.212 315 334 9 | 158.072 205 982 8 | 220.740 852 674 7 | 288.287 832 797 7 |
| 100 000.0 | 31.008 270 700 3 | 111.110 820 964 8 | 218.016 567 608 3 | 340.507 728 578 0 | 475.514 382 764 8 | 621.031 702 467 9 |

[a]Values taken from Ref. [11].
[b]Values taken from Ref. [6].

To show that the wave functions are converging to the exact unbounded ones, in Table II we report some expectation values

$$\langle x^{\alpha}\rangle_i^R=\int_{-R}^{R} dx\, x^{\alpha}|\varphi_i^R(x)|^2 , \tag{5.3}$$

as a function of the size of the interval. They converge smoothly from below to the exact analytical values. Even for highly excited states that are rapidly oscillating, the limit value obtained with the IBA reflects the high quality of the wave function that is provided by the algorithm.

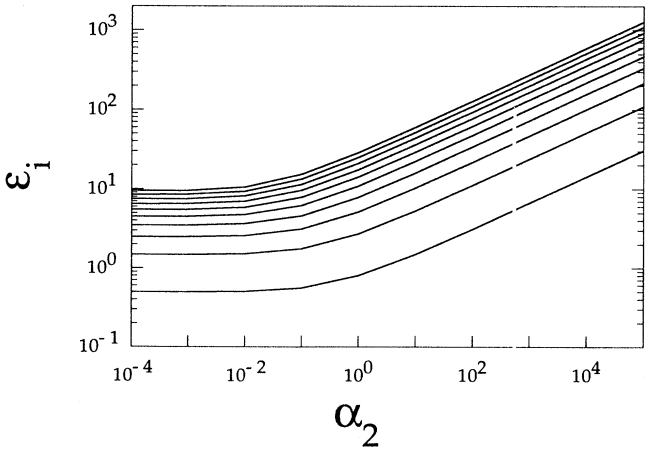


FIG. 4. Variation of the first ten eigenvalues of the unbounded quartic anharmonic oscillator, Eq. (5.4), with respect to the anharmonicity parameter $\alpha_2$.

### B. Anharmonic oscillators: The quartic and sextic potentials

To test the IBA, we have solved the quartic potential

$$V(x)=\tfrac{1}{2}x^2+\alpha_2 x^4 \tag{5.4}$$

for several values of the anharmonicity parameter $\alpha_2$. In Table III we report the eigenvalues of the first six states of the quartic potential for several values of the anharmonicity parameter. Hioe, MacMillen, and Montroll [10] showed that the solutions of this potential can be labeled according to the value of $\alpha_2$. They found three regimes: when $\alpha_2$ is small, the solutions are pure harmonic, when $\alpha_2$ is large, the solutions are classified as pure quartic, and there is a transition zone or boundary layer where the behavior is mixed. In Fig. 4 we depict the variation of the first ten energy levels with the anharmonicity parameter. The behavior obtained with the IBA is the

TABLE IV. First ten eigenvalues for the sextic potential with $\alpha_2=0.5$ and $\alpha_3=1.0$. The step used is $h=0.0025$.

| $n$ | Present work | Ref. [6] |
|---|---|---|
| 1 | 0.874 643 498 6 | 0.874 643 498 6 |
| 2 | 3.111 392 841 6 | 3.111 392 841 6 |
| 3 | 6.197 232 644 1 | 6.197 232 644 2 |
| 4 | 9.932 773 188 8 | 9.932 773 189 2 |
| 5 | 14.206 320 177 7 | 14.206 320 179 0 |
| 6 | 18.953 713 126 8 | 18.953 713 129 7 |
| 7 | 24.129 650 487 2 | 24.129 650 493 0 |
| 8 | 29.699 840 229 8 | 29.699 840 240 5 |
| 9 | 35.637 149 180 7 | 35.637 149 199 1 |
| 10 | 41.919 401 648 1 | 41.919 401 677 8 |

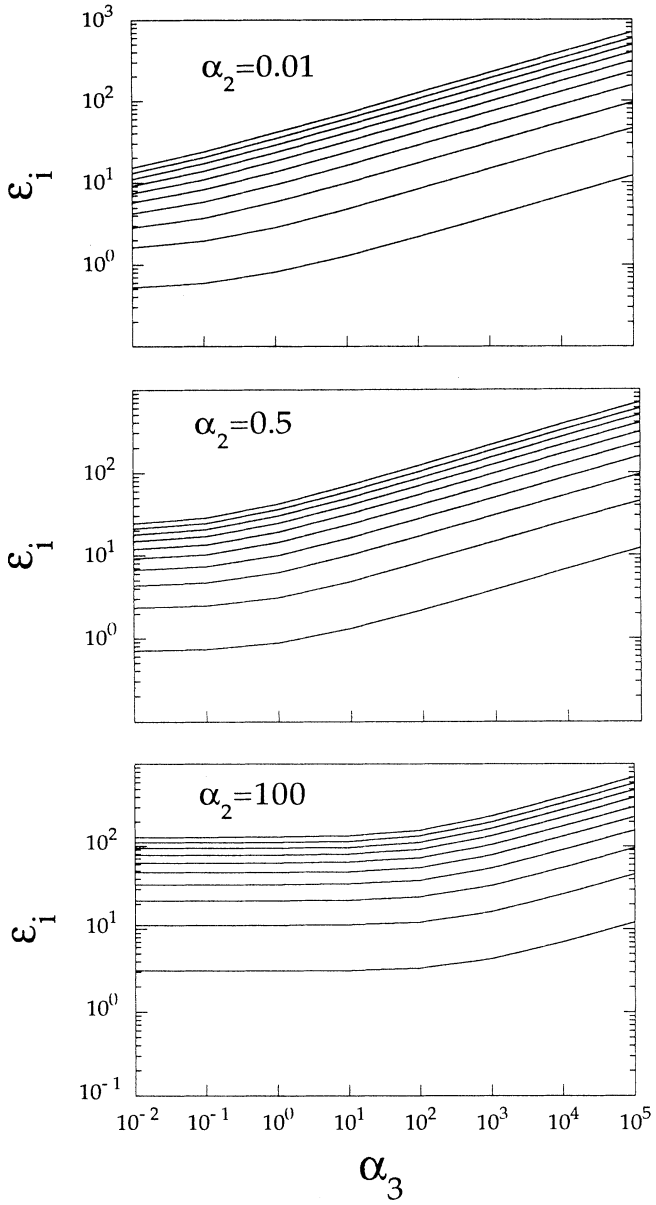


FIG. 5. Variation of the first ten eigenvalues of the unbounded sextic anharmonic oscillator, Eq. (5.5), for different values of the anharmonic parameter $\alpha_2$ and as a function of $\alpha_3$.

same as that reported by Hioe, MacMillen, and Montroll [10]. We would like to stress that with the IBA it is possible to obtain the solutions for any value of the parameter $\alpha_2$. This is in contrast to some numerical techniques that are only applicable for certain values of the anharmonicity parameter.

Finally, we apply the IBA to the sextic potential

$$V(x)=\tfrac{1}{2}x^2+\alpha_2 x^4+\alpha_3 x^6 . \tag{5.5}$$

In Table IV we present the results for the first ten eigenvalues corresponding to the sextic potential with $\alpha_2=0.5$ and $\alpha_3=1.0$. One can see that the values obtained with the IBA are in excellent agreement with those calculated by Aguiar and Xavier [6]. Our values for some of the excited states are slightly lower than those reported by these latter authors. To show the applicability of the IBA, we have calculated the solutions of the sextic potential for a set of $\alpha_2$ values that correspond to each of the different zones (harmonic, boundary, and quartic) found by Hioe, MacMillen, and Montroll [10] in the quartic potential. The results are depicted in Fig. 5. One can see that, similarly to the situation in the quartic potential case, for each value of $\alpha_2$ there are three zones. As this anharmonic contribution increases, the boundary layer moves towards greater values of $\alpha_3$.

## VI. CONCLUSIONS

In this work we have presented a robust and strongly convergent method in the norm of the Hilbert space $L_2(-\infty,\infty)$ to solve one-dimensional quantum problems. By combining a matrix method and an implementation of the increasing boundaries theorems we have shown that one avoids some important disadvantages of other approaches that solve the one-dimensional Schrödinger equation. First, there is no need to provide initial guesses to solve the equation; second, no basis set is required and, third, there is no need to fix a practice infinity. For the bounded harmonic oscillator we have obtained very accurate eigenvalues by means of Richardson's extrapolation. These values can serve as benchmarks for other analytical and numerical techniques. The method has been successfully used to solve the quartic and sextic anharmonic oscillators. Even though the potentials considered in the present work are defined and solved in a symmetric interval, this is not a limitation for the present approach since the method can easily be extended to potentials defined in nonsymmetric intervals. The methodology developed here is also useful to tackle other interesting problems concerned with confined systems, for example, the study of atoms under pressure. Work along these lines is in progress.

## ACKNOWLEDGMENTS

We would like to thank Andres Cedillo for interesting and always fruitful discussions. Financial support for R.V. and J.G. has been partly provided by CONACYT.

[1] S. J. Chang, Phys. Rev. D **12**, 1071 (1975).
[2] E. Bright Wilson, Jr., J. C. Decius, and P. C. Cross, *Molecular Vibrations. The Theory of Infrared and Raman Vibrational Spectra* (Dover, New York, 1955).
[3] C. M. Bender and T. T. Wu, Phys. Rev. **184**, 1231 (1969).
[4] H. H. Aly and A. O. Barut, Phys. Lett. A **145**, 299 (1990).
[5] K. Banerjee and J. K. Bhattacharjee, Phys. Rev. D **29**, 1111 (1984).
[6] M. A. M. de Aguiar and A. L. Xavier, Jr., Phys. Lett. A **164**, 279 (1992).

[7] A. de Souza Dutra, Phys. Lett. A **131**, 319 (1988).
[8] F. M. Fernández, Q. A. Ma, and R. H. Tipping, Phys. Rev. A **40**, 6149 (1989).
[9] I. G. Halliday and P. Suranyi, Phys. Rev. D **21**, 1529 (1980).
[10] F. T. Hioe, D. MacMillen, and E. W. Montroll, Phys. Rep. **43C**, 305 (1978).
[11] C.-S. Hsue and J. L. Chern, Phys. Rev. D **29**, 643 (1984).
[12] R. S. Kaushal, Phys. Lett. A **142**, 57 (1989).
[13] C. S. Lai, Phys. Rev. A **23**, 455 (1981).
[14] P. K. Patnaik, Phys. Lett. A **150**, 269 (1990).
[15] C. A. Singh, S. B. Singh, and K. D. Singh, Phys. Lett. A **148**, 389 (1990).
[16] J. P. Killingbeck, J. Phys. A **20**, 601 (1987).
[17] J. P. Killingbeck and G. Jolicard, Phys. Lett. A **172**, 313 (1993).
[18] H. Taseli, J. Comput. Phys. **101**, 252 (1992).
[19] B. R. Johnson, J. Chem. Phys. **67**, 4086 (1977).
[20] B. R. Johnson, J. Chem. Phys. **69**, 4678 (1978).
[21] J. P. Leroy and R. Wallace, J. Phys. Chem. **89**, 1928 (1985).
[22] B. W. Shore, J. Chem. Phys. **59**, 6450 (1973).
[23] B. G. Wicke and D. O. Harris, J. Chem. Phys. **64**, 5236 (1976).
[24] J. M. Blatt, J. Comput. Phys. **1**, 382 (1967).
[25] F. J. Hajj, J. Phys. B **13**, 4521 (1980).
[26] J. P. Killingbeck, J. Phys. B **15**, 829 (1982).
[27] E. V. Ludeña, J. Chem. Phys. **66**, 468 (1977).
[28] E. Ley-Koo and S. A. Cruz, J. Chem. Phys. **74**, 4603 (1981).
[29] J. L. Marin and S. A. Cruz, J. Phys. B **24**, 2899 (1991).
[30] N. Aquino, Int. J. Quantum Chem. **54**, 107 (1995).
[31] G. A. Arteca, F. M. Fernández, and E. A. Castro, J. Chem. Phys. **80**, 1569 (1984).
[32] M. A. Nuñez, MS thesis, Universidad Autónoma Metropolitana, 1992.
[33] M. A. Nuñez, Phys. Rev. A **47**, 3620 (1993).
[34] M. A. Nuñez and B. G. Izquierdo, Int. J. Quantum Chem. **47**, 405 (1993).
[35] M. A. Nuñez, Int. J. Quantum Chem. **50**, 113 (1994).
[36] M. A. Nuñez, Int. J. Quantum Chem. **51**, 57 (1994).
[37] B. Lindberg, BIT **20**, 486 (1980).
[38] B. Lindberg, J. Chem. Phys. **88**, 3805 (1988).
[39] G. M. Ewing, *Calculus of Variations with Applications* (Dover, New York, 1969).
[40] J. Dieudonné, *Foundations of Modern Analysis* (Academic, New York, 1969).
[41] J. L. Buchanan and P. R. Turner, *Numerical Methods and Analysis* (McGraw-Hill, New York, 1992).